RESEARCH ARTICLES

MITOCHONDRIAL DISEASE

Hypoxia as a therapy for mitochondrial disease

Isha H. Jain,[1,2,3] Luca Zazzeron,[4] Rahul Goli,[1,2,3] Kristen Alexa,[5] Stephanie Schatzman-Bone,[5] Harveen Dhillon,[1,2,3] Olga Goldberger,[1,2,3] Jun Peng,[1,2,3] Ophir Shalem,[3,6,7] Neville E. Sanjana,[3,6,7] Feng Zhang,[3,6,7] Wolfram Goessling,[3,5,8,9] Warren M. Zapol,[4] Vamsi K. Mootha[1,2,3]*

Defects in the mitochondrial respiratory chain (RC) underlie a spectrum of human conditions, ranging from devastating inborn errors of metabolism to aging. We performed a genome-wide Cas9-mediated screen to identify factors that are protective during RC inhibition. Our results highlight the hypoxia response, an endogenous program evolved to adapt to limited oxygen availability. Genetic or small-molecule activation of the hypoxia response is protective against mitochondrial toxicity in cultured cells and zebrafish models. Chronic hypoxia leads to a marked improvement in survival, body weight, body temperature, behavior, neuropathology, and disease biomarkers in a genetic mouse model of Leigh syndrome, the most common pediatric manifestation of mitochondrial disease. Further preclinical studies are required to assess whether hypoxic exposure can be developed into a safe and effective treatment for human diseases associated with mitochondrial dysfunction.

Mitochondria are ancient organelles that are essential for normal physiology and health. The respiratory chain (RC) is crucial to mitochondrial function and generates approximately 90% of cellular adenosine triphosphate (ATP) via oxidative phosphorylation (*1*). In the oxidative step, four large protein complexes transfer electrons from NADH (the reduced form of nicotinamide adenine dinucleotide) or FADH (the reduced form of flavin adenine dinucleotide) to oxygen while generating a proton gradient. Approximately 90% of the oxygen we breathe is used as a substrate for the RC (*1*). In the phosphorylation step, the proton gradient is dissipated by a fifth and final complex to generate ATP. Numerous additional chemical reactions and transport processes are intimately coupled to the redox and proton-pumping activities of the RC.

A spectrum of human diseases result from a faulty RC (*2*–*4*). Virtually all age-related disorders, including type 2 diabetes, neurodegeneration, and sarcopenia, are accompanied by a quantitative decline in the activity of the mitochondrial RC. The aging process itself is associated with a gradual decrease of oxidative phosphorylation in multiple tissues. Monogenic disorders of the mitochondrial RC represent the largest class of inborn errors of metabolism. To date, lesions in over 150 genes, encoded by the nuclear or mitochondrial (mtDNA) genomes, have been identified as disease-causing. Mutations in these genes lead to a biochemical deficiency of one or more of the RC complexes, resulting in either tissue-specific or multisystem disease with devastating effects on human health. Patients with RC disorders can present with blindness, deafness, gray- or white-matter brain disease, cardiomyopathy, skeletal muscle myopathy, gastrointestinal dysmotility, anemia, ataxia, liver disease, and kidney disease.

Management of these disorders remains challenging (*5*, *6*). Although individual mutations are rare, the overall disease burden of mitochondrial disease is significant, with an estimated prevalence of 1 out of 4300 live births (*7*). Therefore, a general and effective therapeutic is needed. The current mainstay of managing mitochondrial disease involves the use of vitamin cofactors (such as coenzyme Q, α-lipoic acid, riboflavin, or L-carnitine) (*8*). Other proposed strategies include the use of small-molecule bypass of defective RC components, using electron carriers such as idebenone, and antioxidants. None of these approaches have demonstrated efficacy in randomized controlled clinical trials.

Several lines of evidence point to the existence of endogenous coping mechanisms for dealing with mitochondrial dysfunction. Mitochondrial disorders can be highly tissue-specific and episodic (*2*, *9*). These disorders are often triggered by drugs, alcohol, or viral illnesses, implying that a genetic lesion is not always sufficient to cause cellular dysfunction, but rather that the lesion may need to be compounded with an environmental insult. Such observations suggest the existence of cellular pathways or environments that buffer against mitochondrial lesions.

A genome-wide screen to spotlight suppressors of mitochondrial disease

We modeled mitochondrial disease in the human leukemic suspension cell line K562 and performed a Cas9-mediated knockout (KO) screen (*10*, *11*). We used the natural product antimycin as a complex III inhibitor of the RC. In the presence of antimycin, the RC is unable to oxidize high-energy reducing equivalents to power ATP production; however, cytoplasmic lactate dehydrogenase maintains NAD^+ redox balance. Removal of pyruvate exacerbates reductive stress, further preventing cell proliferation (*12*). We modeled mitochondrial disease with the addition of antimycin alone (moderate disease) or antimycin in combination with the removal of pyruvate (severe disease), using cell growth as a proxy for disease magnitude (Fig. 1A). We infected K562 cells with a ~65,000 single-guide RNA (sgRNA) library, targeting ~18,000 genes (*10*). After 1 week of genome editing, we transferred the pool of KO cells to experimental conditions of untreated, moderate disease, and severe disease states (Fig. 1B). We collected samples for an enrichment screen by allowing the KO pool to grow in selection conditions for 3 weeks. The relative growth between untreated and moderate disease conditions was 300-fold and between untreated and severe disease conditions was 7000-fold (Fig. 1C).

As expected, 3 weeks of genome editing in untreated cells led to a significant depletion of sgRNAs corresponding to essential genes, including those related to transcription, translation, and splicing (fig. S1). Nearly 20% of the 500 most essential genes were mitochondrial proteins, especially mitochondrial ribosomal proteins and electron transport chain subunits (table S1). Because mitochondrial proteins make up approximately 5% of the proteome (*13*), this enrichment highlights the dramatic effects of mitochondrial dysfunction on viability.

Of the ~18,000 genes tested, the KO screen identified inhibition of the Von Hippel-Lindau (VHL) factor as the most effective genetic suppressor of mitochondrial disease, in both the moderate and severe disease conditions (Fig. 1D). RIGER analysis ranked VHL KO cells as the most enriched over time in both infection replicates corresponding to severe and moderate disease (table S2). The five sgRNAs spanning all three exons of VHL ranked 1, 2, 3, 12, and 14 out of ~65,000 total guides for enrichment in disease conditions relative to pretreatment conditions (Fig. 1, D to F, and figs. S2 and S3). Furthermore, the most significant VHL sgRNAs were enriched approximately 20-fold in disease states (fig. S4). VHL KO cells were also enriched in untreated conditions over time, reflecting an overall effect on cell growth. However, this enrichment was significantly less than in disease conditions.

[1]Department of Molecular Biology and Howard Hughes Medical Institute, Massachusetts General Hospital, Boston, MA, USA. [2]Department of Systems Biology, Harvard Medical School, Boston, MA, USA. [3]Broad Institute of Harvard and MIT, Cambridge, MA, USA. [4]Department of Anesthesia, Critical Care, and Pain Medicine, Massachusetts General Hospital, Boston, MA, USA. [5]Genetics Division, Brigham and Women's Hospital, Harvard Medical School, Boston, MA, USA. [6]McGovern Institute for Brain Research, Cambridge, MA, USA. [7]Department of Brain and Cognitive Sciences and Department of Biological Engineering, Massachusetts Institute of Technology, Cambridge, MA, USA. [8]Gastrointestinal Cancer Center, Dana-Farber Cancer Institute, Boston, MA, USA. [9]Harvard Stem Cell Institute, Cambridge, MA, USA.
*Corresponding author. E-mail: vamsi@hms.harvard.edu

VHL activity is a key regulator of the hypoxic response pathway (*14*, *15*). Organisms have evolved elaborate mechanisms to adapt to fluctuating oxygen tensions and extreme environments. In normoxic conditions, the hypoxia-inducible transcription factors (HIFs) are constitutively made and hydroxylated by the prolyl-hydroxylase (PHD) enzymes (Fig. 2A) (*16*–*18*). The hydroxylated form is recognized by the ubiquitin ligase, VHL, and targeted for degradation. In response to environmental hypoxia, the PHD reaction does not take place, allowing HIF stabilization and activation of the hypoxia transcriptional program (Fig. 2B). VHL KO cells show HIF stabilization, even during normoxic conditions, thereby bypassing cellular oxygen-sensing mechanisms (*18*–*20*). Our screen suggested that harnessing innate responses to hypoxia may be protective in the setting of inherited mitochondrial disease.

Genetic and small-molecule proof of concept in cellular models

We validated and characterized the hypoxic response as a therapeutic target by testing the ability of VHL KO cells to withstand respiratory-chain dysfunction. VHL KO cells showed increased cell proliferation in the presence of antimycin relative to nontargeting (dummy) sgRNA-modified cells (Fig. 2C). Furthermore, there was perfect correspondence between the degree of VHL sgRNA enrichment in the CRISPR (clustered regularly-interspaced short palindromic repeats) screen and the rescue-effect size of individual sgRNAs (fig. S5). VHL KO cells were also more resistant to complex I inhibition by piericidin and complex V (ATP synthase) inhibition by oligomycin, demonstrating the potentially broad utility of our therapeutic approach (Fig. 2C).

We next explored small molecules as tools for triggering the hypoxia response. Although a VHL inhibitor has been reported (*21*), it is not cell-permeant. PHD inhibitors have been developed as investigational drugs for anemia and ischemic disorders (*22*). FG-4592 is currently in phase III clinical trials for the treatment of anemia of chronic kidney disease and acts by upregulating the canonical marker of the hypoxia response, erythropoietin (Epo). We reasoned that FG-4592 treatment would mimic VHL KO, thus triggering a broader hypoxia transcriptional program. Normal growth rates were minimally increased by FG-4592. Complex I, III, or V inhibition stunts cell growth but does not increase cell death (fig. S6) in most cell lines, including HT-29s, HEK 293Ts, and K562s. Administering ~50 μM FG-4592 in advance and during RC dysfunction nearly or completely rescued this growth defect, in a dose-dependent manner (Fig. 2, D to F, and fig. S7). The nearly full rescue of the disease state across different cell lines and across chemical lesions highlights the general utility of our approach.

We characterized the rescue mechanism of FG-4592 by studying its effect on the hypoxia response and energy metabolism. Although HIF1α is undetectable during normoxic exposure, treatment with FG-4592 stabilized the transcription factor even during normoxia. It has previously been noted that a paradox exists between severe mitochondrial dysfunction and cellular sensing of hypoxia (*23*). In cell culture, full inhibition of the RC prevents HIF stabilization,

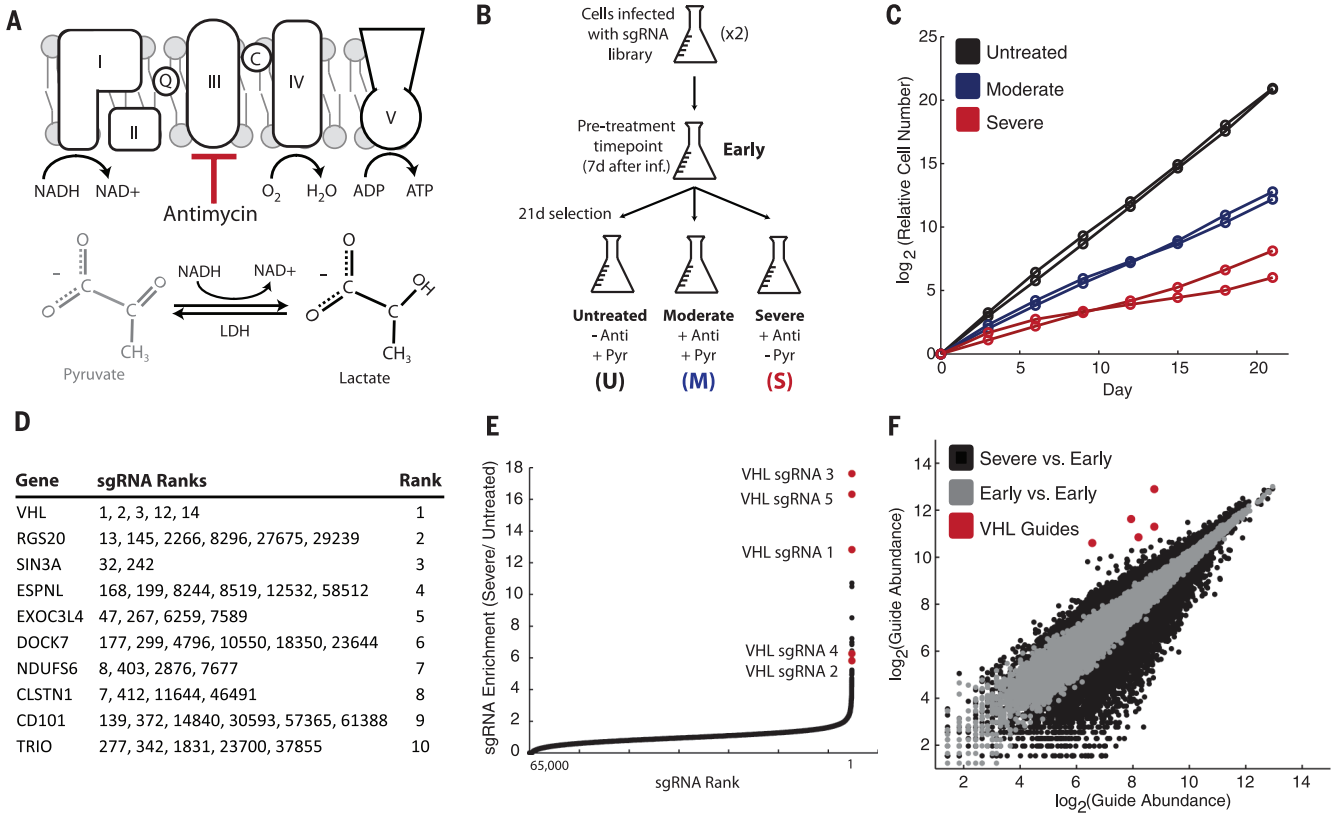

Gene	sgRNA Ranks	Rank
VHL	1, 2, 3, 12, 14	1
RGS20	13, 145, 2266, 8296, 27675, 29239	2
SIN3A	32, 242	3
ESPNL	168, 199, 8244, 8519, 12532, 58512	4
EXOC3L4	47, 267, 6259, 7589	5
DOCK7	177, 299, 4796, 10550, 18350, 23644	6
NDUFS6	8, 403, 2876, 7677	7
CLSTN1	7, 412, 11644, 46491	8
CD101	139, 372, 14840, 30593, 57365, 61388	9
TRIO	277, 342, 1831, 23700, 37855	10

Fig. 1. Genome-scale Cas9-mediated knockout screen identifies VHL inhibition as protective during states of mitochondrial dysfunction. (**A**) Mitochondrial disease was modeled with the addition of the complex III inhibitor antimycin (moderate disease) or addition of antimycin and removal of pyruvate (severe disease). (**B**) K562 cells were infected in duplicate with the genome-scale Cas9-mediated knockout library and separated into conditions of untreated, moderate disease, or severe disease. Samples were taken at a pretreatment time point, as well as after 3 weeks of selection. (**C**) Growth curves for cumulative differences in growth rates in different experimental conditions for both infection replicates. (**D**) RIGER output based on enrichment of sgRNAs in severe disease condition relative to pretreatment conditions. Each row denotes a single gene, with ranks of corresponding sgRNAs in the middle column. Ranks for individual sgRNAs are out of ~65,000 total sgRNAs in the library. (**E**) sgRNA enrichment magnitude versus rank, with most enriched sgRNA shown at the far right. sgRNAs corresponding to VHL are in red. (**F**) Guide abundance in pretreatment conditions (infection 1 versus infection 2) shown in gray for each sgRNA, representative of experimental noise. Guide abundance in severe disease condition versus pretreatment condition is in black, with VHL sgRNAs in red.

even under low oxygen conditions that would otherwise trigger the hypoxia response (*23*, *24*). FG-4592 treatment bypassed this paradox and enabled HIF1α stabilization in the face of mitochondrial dysfunction, during states of normoxia or hypoxia (Fig. 3A). Further work is needed to determine whether the paradox contributes significantly to disease pathology or whether it is simply a feature of severe RC blockade in cultured cells.

The HIF transcriptional response is believed to be protective during states of hypoxia, at least in part by shifting the cell's reliance away from mitochondrial oxidative energy metabolism. The HIF1α response can preserve energy supply at low oxygen tensions in a redox-neutral manner. Indeed, treatment with FG-4592 for 24 hours up-regulated the transcription of glycolytic enzymes (Fig. 3B and fig. S8) such as glucose transporter 1 (GLUT1), hexokinase 2 (HK2), and lactate dehydrogenase A (LDHA). HIF1α activation is also known to shunt the carbon supply away from the TCA cycle and toward the LDHA reaction (*25*–*28*), as evidenced by the significant up-regulation of pyruvate dehydrogenase kinase (PDK1) (Fig. 3B). Although lesions to the RC and hypoxia can in principle limit RC activity, cells do not mount the hypoxia response upon RC inhibition, because the signal is lacking. However, FG-4592 treatment artificially triggers the hypoxia transcriptional program, even during normoxic conditions (Fig. 3B and fig. S8).

To corroborate the transcriptional changes, we also measured lactic acid production and oxygen consumption as proxies of glycolysis and oxidative phosphorylation. Glycolysis was somewhat increased by RC inhibition, probably as a result of allosteric mechanisms (Fig. 3C). Treatment with FG-4592 increased glycolysis by nearly 25% in HEK293T cells under basal conditions and beyond allosteric mechanisms in response to RC inhibition. Furthermore, basal oxygen consumption was decreased by approximately twofold with FG-4592 treatment (Fig. 3D). This may be protective in the setting of mitochondrial dysfunction, because it may limit the amount of reactive oxygen species (ROS) produced by impaired electron transport.

Genetic and small-molecule proof of concept in zebrafish models

To further establish proof of concept, we asked whether genetic or small-molecule activation of the hypoxia response would be protective against RC poisoning in zebrafish embryos. *vhl*-null zebrafish continuously up-regulate the hypoxia response throughout early development (*29*). Just as *vhl* KO cells are protected against mitochondrial dysfunction, we asked whether *vhl*-null zebrafish might be more resilient to RC poisoning. Zebrafish

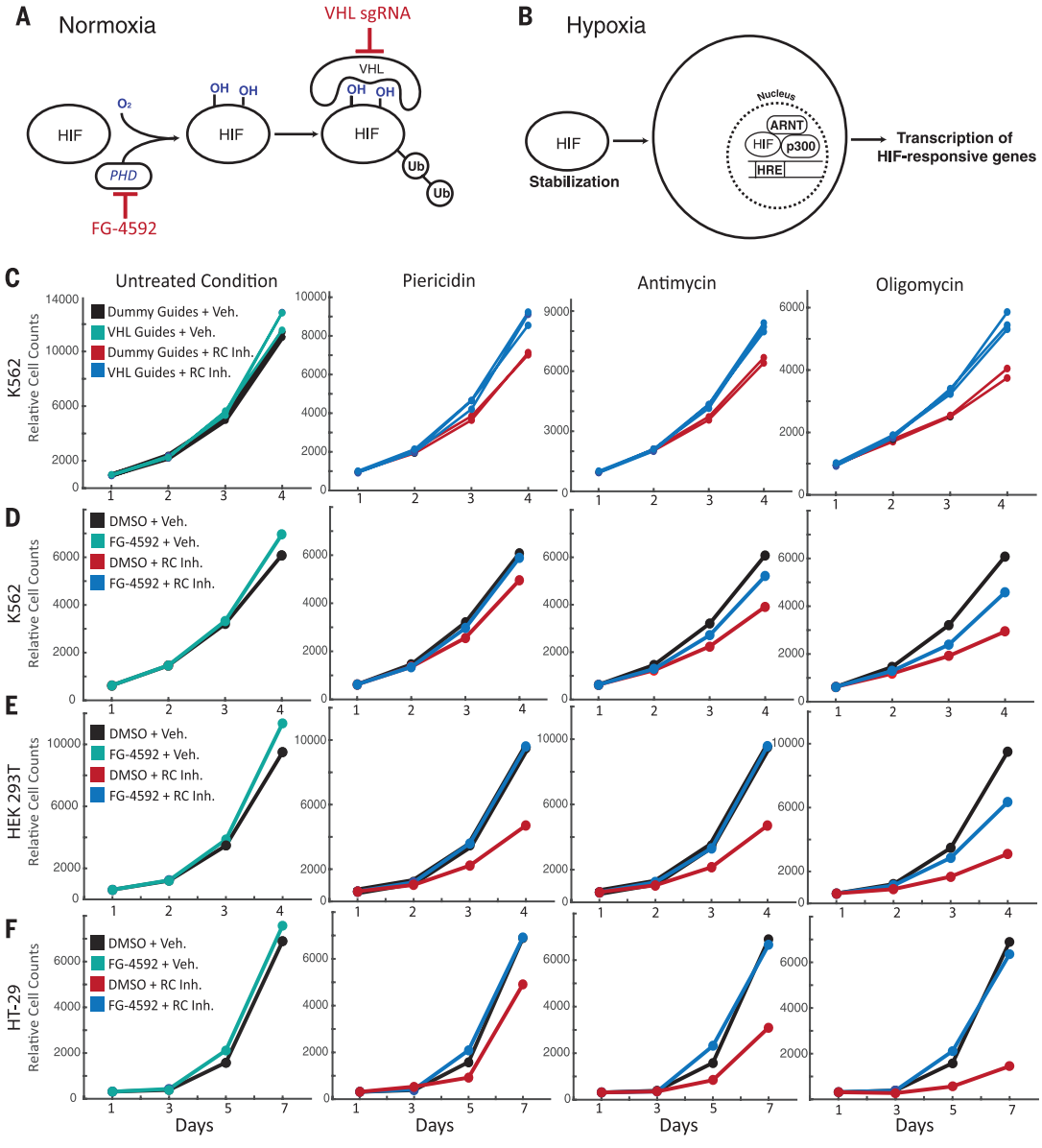

Fig. 2. Genetic or small-molecule activation of the HIF response is protective against multiple forms of RC inhibition, in multiple cell types. (**A**) Schematic for HIF degradation during normoxia. (**B**) Schematic for induction of hypoxia transcriptional program during hypoxia. (**C**) Growth curves for K562 VHL KO cells (cyan and blue) or nontargeting sgRNA cells (black and red) for untreated or disease conditions (the mean is shown). Disease conditions correspond to inhibition of complex I (piericidin), complex III (antimycin), or complex V (oligomycin). Growth curves for (**D**) K562 cells, (**E**) HEK293T cells, and (**F**) HT-29 cells ± FG-4592, in combination with untreated or disease conditions (inhibition of complexes I, III, and V), are shown. All time points were measured in duplicate, and all growth curves are representative of two or three independent experiments (the mean is shown). All final cell counts of FG-treated rescue [or VHL KO rescue in (A)] in the presence of RC inhibitor were statistically significant (one-sided *t* test *P* value < 0.05).

embryos exhibit sensitivity to multiple specific RC inhibitors, including antimycin (*30*–*32*). We demonstrated a significant improvement in the survival of *vhl*-null embryos exposed to 2.5 nM antimycin as compared to heterozygous and wild-type (WT) controls (Fig. 4A).

We then extended our small-molecule approach to the zebrafish model of RC dysfunction. A previously generated zebrafish reporter strain, Tg (*phd3::EGFP*), expresses green fluorescent protein (GFP) under the control of a HIF-responsive promoter, thereby enabling in vivo assessment of activating the hypoxia transcriptional response (*33*, *34*). FG-4592 treatment of Tg(*phd3::EGFP*) embryos at 96 hours post fertilization (hpf) resulted in a time-dependent increase in the fluorescence of individual reporter fish (Fig. 4B). Furthermore, in situ hybridization for the glycolytic HIF targets *glut1* and *ldha1* demonstrated significant up-regulation upon FG-4592 treatment (Fig. 4C), confirming that FG-4592 engages the zebrafish PHDs to trigger the hypoxia transcriptional program. We then demonstrated that cotreatment of embryos with FG-4592 rescued antimycin-induced death by nearly twofold (Fig. 4D). The genetic and small-molecule experiments in zebrafish provide proof of concept that activation of the hypoxia program can protect against insults to the mitochondrial RC.

Hypoxic breathing alleviates disease and extends life span in a mouse model of Leigh syndrome

The cellular and zebrafish models provided proof of the concept that individual components of the cellular response to hypoxia are protective

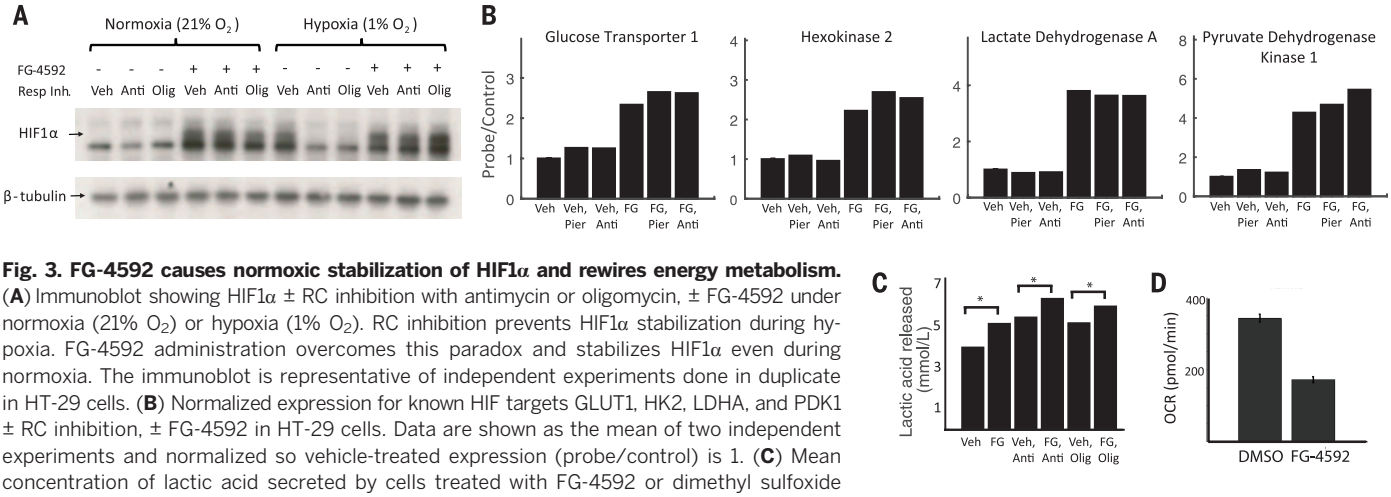

Fig. 3. FG-4592 causes normoxic stabilization of HIF1α and rewires energy metabolism. (**A**) Immunoblot showing HIF1α ± RC inhibition with antimycin or oligomycin, ± FG-4592 under normoxia (21% O_2) or hypoxia (1% O_2). RC inhibition prevents HIF1α stabilization during hypoxia. FG-4592 administration overcomes this paradox and stabilizes HIF1α even during normoxia. The immunoblot is representative of independent experiments done in duplicate in HT-29 cells. (**B**) Normalized expression for known HIF targets GLUT1, HK2, LDHA, and PDK1 ± RC inhibition, ± FG-4592 in HT-29 cells. Data are shown as the mean of two independent experiments and normalized so vehicle-treated expression (probe/control) is 1. (**C**) Mean concentration of lactic acid secreted by cells treated with FG-4592 or dimethyl sulfoxide (DMSO) ± RC inhibitors as proxy for anaerobic glycolytic flux. Data are shown for HEK293T cells (without pyruvate to eliminate a contribution from the LDHA reaction) and are representative of at least two independent experiments. (**D**) Basal oxygen consumption rates for HEK293T cells treated with FG-4592 or DMSO for >24 hours, averaged across three independent experiments (mean ± SE) [one-sided *t* test *P* value < 0.05 for all pairwise comparisons ± FG-4592 in (B) to (D)]. OCR, oxygen consumption rate.

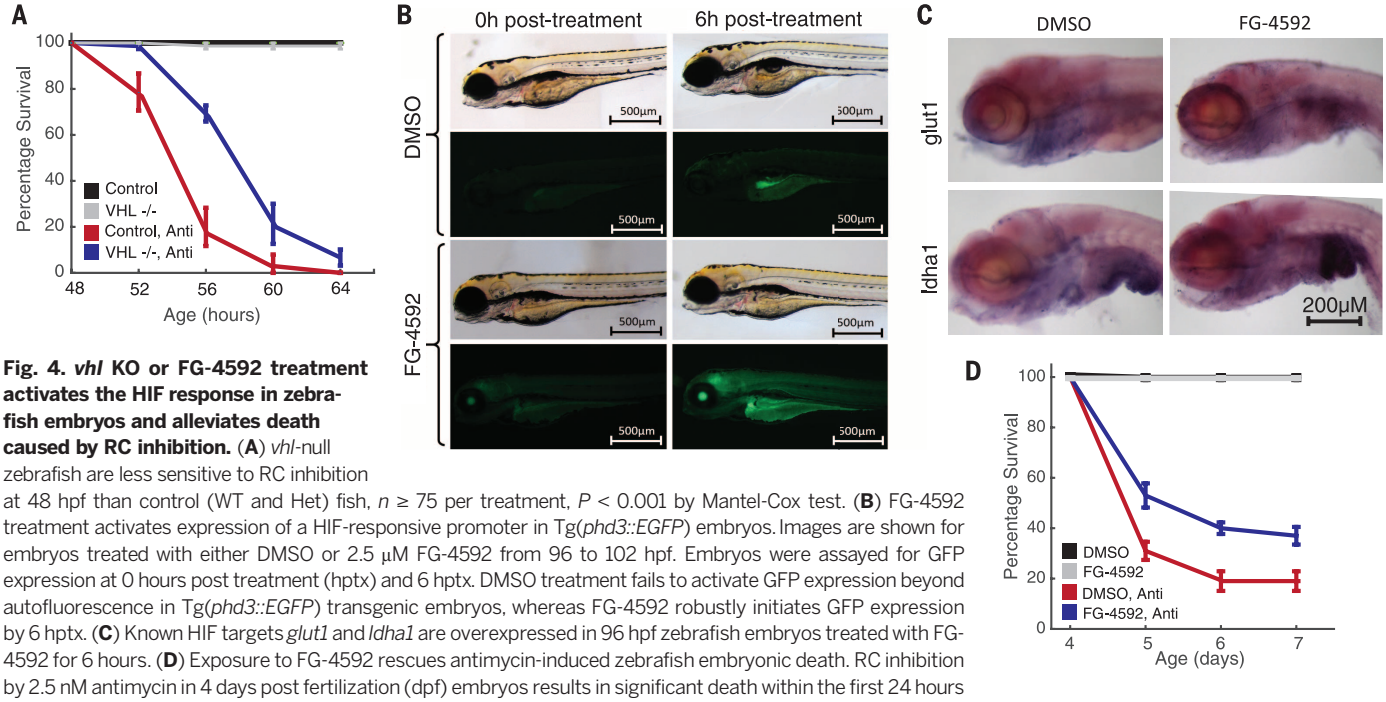

Fig. 4. *vhl* KO or FG-4592 treatment activates the HIF response in zebrafish embryos and alleviates death caused by RC inhibition. (**A**) *vhl*-null zebrafish are less sensitive to RC inhibition at 48 hpf than control (WT and Het) fish, $n \geq 75$ per treatment, $P < 0.001$ by Mantel-Cox test. (**B**) FG-4592 treatment activates expression of a HIF-responsive promoter in Tg(*phd3::EGFP*) embryos. Images are shown for embryos treated with either DMSO or 2.5 μM FG-4592 from 96 to 102 hpf. Embryos were assayed for GFP expression at 0 hours post treatment (hptx) and 6 hptx. DMSO treatment fails to activate GFP expression beyond autofluorescence in Tg(*phd3::EGFP*) transgenic embryos, whereas FG-4592 robustly initiates GFP expression by 6 hptx. (**C**) Known HIF targets *glut1* and *ldha1* are overexpressed in 96 hpf zebrafish embryos treated with FG-4592 for 6 hours. (**D**) Exposure to FG-4592 rescues antimycin-induced zebrafish embryonic death. RC inhibition by 2.5 nM antimycin in 4 days post fertilization (dpf) embryos results in significant death within the first 24 hours of treatment. Coexposure of antimycin with FG-4592 (2.5 μM) doubles embryo survival, whereas FG-4592 alone has no impact. $n = 75$ embryos per treatment, $P < 0.0001$ by Mantel-Cox test.

against mitochondrial toxins. Although small molecules are capable of activating specific branches of the hypoxia program, we reasoned that they may not have as broad and potent an effect as the naturally evolved, whole-body physiological response to hypoxia itself. Moreover, small-molecule drugs for activating the hypoxia response are currently in clinical trials for kidney disease and anemia. However, a large fraction of mitochondrial disease originates in the central nervous system, and our preliminary pharmacokinetic studies suggested limited blood-brain barrier penetration of these drugs in mice. Higher doses resulted in whole-body toxicity. Because mammals have evolved a complex homeostatic program to adapt to low oxygen tensions in their environment, we reasoned that a similarly broad hypoxic stress response might protect animal models of mitochondrial disease.

Leigh syndrome is the most common pediatric form of mitochondrial disease. Though relatively healthy at birth, patients develop irreversible neurodegeneration by 2 years of age (*6*). They suffer bilaterally symmetric lesions in the brain stem and basal ganglia, with marked gliosis. Most patients die between the ages of 3 and 16 months. To date, over 75 different genes have been implicated in this syndrome, with complex I deficiency being the most frequent biochemical cause of disease. One of the more severe recessive forms of Leigh syndrome is caused by inactivation of the *NDUFS4* gene, which codes for NADH:ubiquinone oxidoreductase subunit S4. Recently, a mouse model that recapitulates many features of Leigh syndrome was generated by disruption of the murine *Ndufs4* gene (*35*). *Ndufs4* KO mice breathing ambient air (21% O_2) display retarded growth rates, impaired visual acuity, and a delayed startle response. Their body temperature falls progressively until reaching 32°C, shortly before death at 50 to 60 days of age. Diseased mice also display locomotor deficits and failure to thrive by 50 days of age. Their neuropathology closely resembles clinical findings, with a substantial inflammatory response in the brainstem and cerebellum.

We first performed experiments to confirm that *Ndufs4* KO mice can tolerate a brief exposure to environmental hypoxia and that they activate a hypoxic response in a manner similar to WT mice. We exposed four WT mice and four KO mice to 8.5% O_2 at sea-level pressure for 6 hours. Acute exposure of WT mice to hypoxia triggers HIF stabilization, resulting in Epo transcription and translation. After a 6-hour exposure, we measured Epo protein levels in plasma and showed that both WT and KO mice up-regulated Epo production by approximately 40-fold (fig. S9). These results

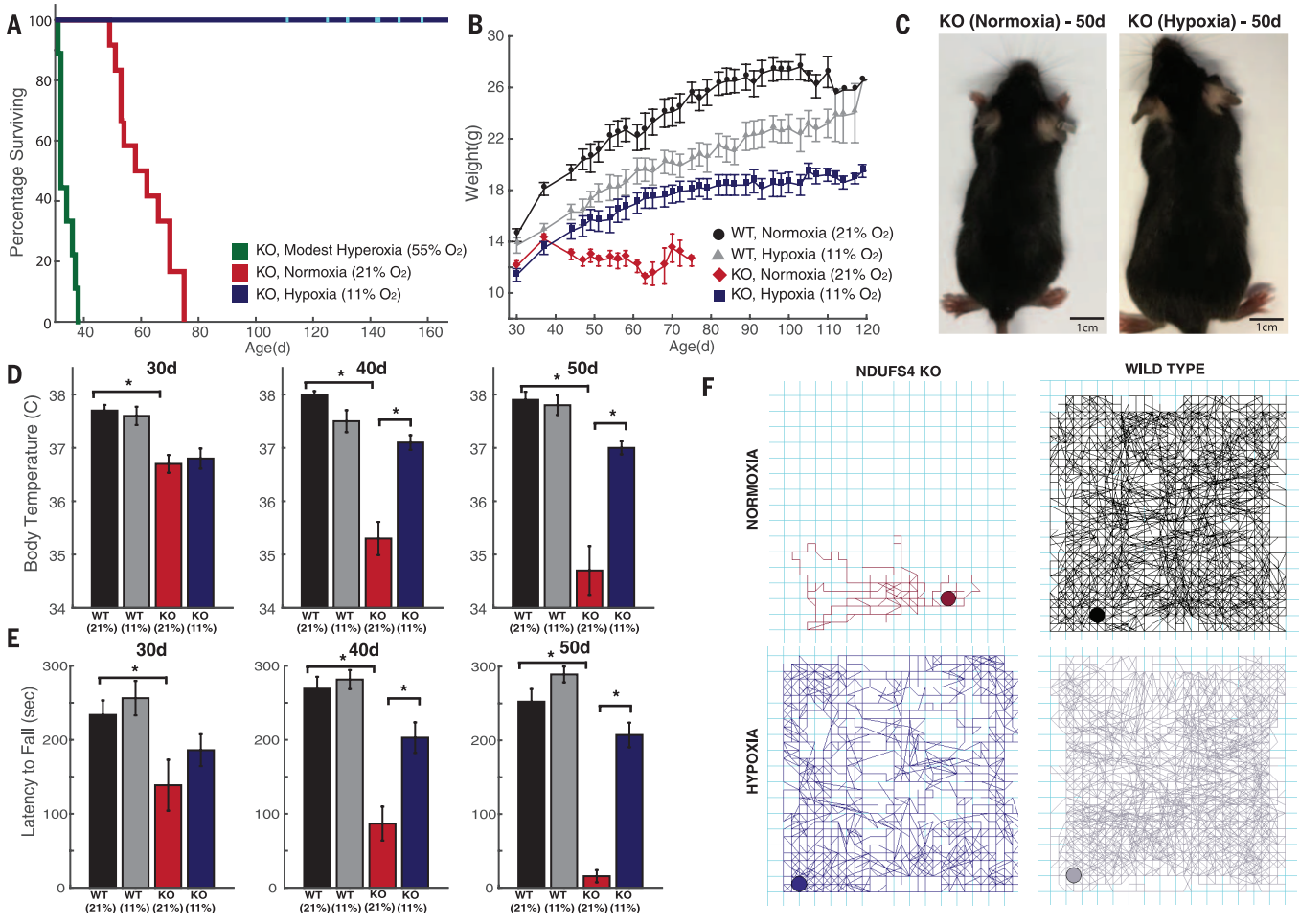

Fig. 5. Chronic hypoxia extends life span and alleviates disease in a mouse model of Leigh syndrome, whereas chronic hyperoxia exacerbates disease. (**A**) *Ndufs4* KO mice of both genders were chronically exposed to hypoxia (11% O_2), normoxia (21% O_2), or hyperoxia (55% O_2), at 30 days of age and survival was recorded (n = 12, n = 12, n = 9 mice, respectively). Cyan bars represent the current age of hypoxic KO mice. (**B**) Body weights were measured in WT and KO mice exposed to normoxia or hypoxia, three times a week upon enrollment in the study. Weights are shown as mean ± SE. (**C**) Representative images of 50-day-old KO mice exposed to normoxia or hypoxia. (**D**) Body temperature was measured in KO mice exposed to normoxia or hypoxia at age ~30, 40, and 50 days. Temperatures are shown as mean ± SE ($n \geq 7$ mice for all groups). (**E**) Latency to fall on an accelerating rod was measured as median values of triplicate trials per mouse for WT and KO mice, exposed to normoxia or hypoxia at different ages ($n \geq 7$ mice for all groups). (**F**) Representative 1-hour locomotor activity traces of sick, normoxia-treated KO mice, and age-matched hypoxia-treated KO mice, as well as controls. All data are shown as normoxia KO (maroon), hypoxia KO (blue), normoxia WT (black), and hypoxia WT (gray). *Denotes t test P value < 0.05.

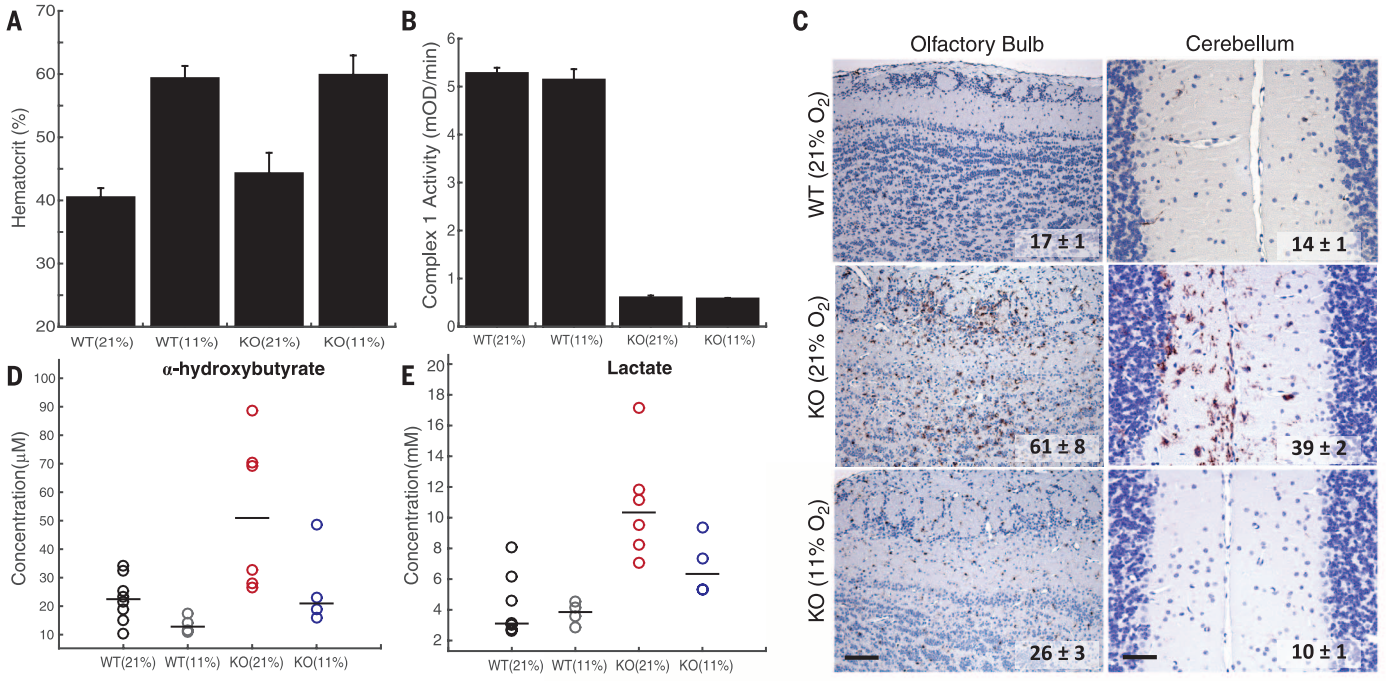

Fig. 6. Hypoxia exposure of *Ndufs4* KO mice alleviates metabolic disease markers, as well as neuropathology, without rescuing complex I activity. (**A**) Hematocrit values for WT and KO mice treated with normoxia or hypoxia for ~3 weeks (n = 3 or 4 mice per group, test P value < 0.05 for normoxia versus hypoxia for both WT and KO). (**B**) Complex I activity is significantly reduced in KO mice relative to WT mice, in both normoxic and hypoxic conditions (n = 3 or 4 mice per group, t test P value < 0.01). mOD, milli–optical density. (**C**) Representative images for immunostaining against the inflammatory marker Iba-1 in the olfactory bulb and cerebellum of *Ndufs4* KO mice treated with hypoxia or normoxia and WT mice exposed to normoxia breathing. The number of Iba-1–positive cells per 10 random fields of view is shown for each treatment group (mean ± SE, t test P value < 0.01 for normoxic versus hypoxic KO, n = 3 or 4 mice per group). Scale bar, 200 μm for the olfactory bulb and 50 μm for the cerebellum. (**D**) Plasma α-HB levels in WT and KO mice exposed to hypoxia or normoxia (n = 4 to 8 mice per group). The median is shown as a horizontal bar. (**E**) Plasma lactate in WT and KO mice exposed to hypoxia or normoxia (n = 4 to 8 mice per group). The median is shown as a horizontal bar.

indicate that the KO mice mount a hypoxic transcriptional response and that the RC inhibition–HIF stabilization paradox does not extend to this disease setting.

We next tested whether chronic exposure to moderate environmental hypoxia [breathing 11% O_2, a level known to be tolerated by humans (equivalent to 4500 m altitude)] could alleviate the disease phenotype in the *Ndufs4* KO mice. Environmental hypoxia was generated by adjusting the relative concentration of nitrogen and oxygen in the input gas mixture. This created environmental oxygen tensions similar to those found in the high mountain communities of Nepal and Peru (*36*). Continuous gas flow and CO_2 absorption by $Ca(OH)_2$ within the 11% O_2 hypoxic chamber maintained CO_2 levels below 0.4% with continuous monitoring. A control ambient environment for breathing 21% O_2 was created with an identical chamber setup. *Ndufs4* KO and control mice were continuously exposed to breathing at normoxia or 11% hypoxia after enrollment in the experiment, excluding brief exposure to normoxia for behavior tests and maintenance three times per week. Untreated *Ndufs4* KO mice typically began to show disease progression after approximately 30 days of post-birth air exposure, which is about 10 days after weaning. Because hypoxia-related vascular responses (constriction of pulmonary circulation and dilation of the ductus arteriosus) occur in early postnatal development, we initiated chronic hypoxic exposure treatments after the mice were 30 days old.

Remarkably, chronic hypoxia prevented the development of many disease symptoms in the *Ndufs4* KO mice and significantly extended their survival. All normoxia-exposed *Ndufs4* KO mice either fulfilled criteria for humane euthanasia or died at a median age of ~60 days, with none surviving past 75 days (Fig. 5A). In contrast, there were no deaths in *Ndufs4* KO mice that were chronically breathing 11% O_2. Several mice showed a mild clasping phenotype at ages greater than 120 days. At the time of submission of this manuscript, the oldest KO mice breathing 11% O_2 were 170 days old.

Hypoxia-treated mice showed an improvement in body weight gain, core temperature maintenance, and neurologic behavior. All *Ndufs4* KO mice continued to gain weight between 30 and 37 days of age (Fig. 5, B and C). At this stage, untreated KO mice lose weight, become hypothermic, and die. In contrast, *Ndufs4* KO mice breathing 11% O_2 gained weight for several weeks, at which point body weight gain slowed, similar to the growth kinetics of WT mice. The growth rate of hypoxia-treated KO mice matched that of WT mice breathing 11% O_2 upon treatment, suggesting that the primary cause of weight loss was alleviated by hypoxic exposure. At 30 days of age, untreated *Ndufs4* KO mice had similar core body temperatures to control mice. However, by 50 days there was nearly a 4°C drop in temperature (Fig. 5D). KO mice chronically breathing 11% O_2 showed no reduction of core body temperature. Thus, chronic hypoxic breathing improves the underlying metabolic phenotype that directly or indirectly results in alterations of energy and nutrient metabolism.

Ndufs4 KO mice, as well as patients suffering from Leigh syndrome, exhibit striking defects in locomotor activity. Ataxia and failure to thrive are hallmarks of mitochondrial dysfunction. Behavioral tests were performed at 10-day intervals in normoxia and hypoxia-treated WT and KO mice. The rotarod test (*37*) measures the ability of mice to maintain grip strength and balance and resist fatigue on an accelerating rotating rod. At 30 days of age, KO mice breathing air displayed a slight depression in the median time that they could stay on a rotarod (Fig. 5E). This ability declined by 40 days, and at 50 days, untreated KO mice were no longer able to stay on the rod for more than a few seconds, due to a combination of muscular weakness, inability to balance, and loss of visual acuity. Hypoxia-treated WT mice performed similarly to normoxia-treated control mice. KO mice breathing 11% O_2 displayed a near-complete rescue of this locomotor phenotype. As a further neurological behavioral

test, spontaneous locomotor activity was measured as total distance traveled within an hour (Fig. 5F). Untreated KO mice showed drastically reduced spontaneous locomotor activity and jump counts. These defects were rescued in hypoxia-treated mice, although only to 50% of the values of normoxic WT mice (fig. S10).

Modest hyperoxic breathing exacerbates disease in a mouse model of Leigh syndrome

The striking therapeutic effect of hypoxia led us to investigate whether oxygen itself was a key molecular parameter determining Leigh syndrome progression. Thus, we asked whether the converse environmental scenario of chronic mild hyperoxic exposure (55% O_2) would affect the disease. We exposed WT and *Ndufs4* KO mice to 55% normobaric oxygen starting at 30 days of age. We found that breathing 55% oxygen had no effect on the survival of the WT mice. In contrast, all *Ndufs4* KO mice breathing 55% oxygen died within 2 to 11 days of this exposure; this is significantly earlier than *Ndufs4* KO mice breathing ambient air (21% O_2), which typically succumb within 3 to 4 weeks after experimental exposures begin (Fig. 5A). The reduced survival of the KO mice breathing 55% O_2, along with the markedly extended health span of the KO mice that were breathing 11% O_2, points to the essential and previously unappreciated role of arterial oxygen tension in determining the progression of mitochondrial disease. This suggests that patients with mitochondrial disease may be highly sensitive to oxygen toxicity.

Circulating biomarkers and histopathology in a hypoxia-treated mouse model of Leigh syndrome

We further characterized *Ndufs4* KO mice after treatment with chronic hypoxia. As expected, the hematocrit in these mice was elevated from 40% during normoxia to ~60% during hypoxia, indicating EPO target engagement by hypoxic breathing (Fig. 6A). Given how effective hypoxia is in treating these mice, we asked whether they still retained a deficiency in complex I activity. Indeed, we found that although *Ndufs4* KO mice appeared healthy after hypoxia treatment, brain complex I activity remained dramatically reduced to the same levels as in untreated *Ndufs4* KO mice (Fig. 6B).

Normoxia-treated KO mice exhibited substantial neuronal degeneration. Lesions were accompanied by Iba-1$^+$ microglial proliferation within the olfactory lobes, cerebellum, and brainstem, as documented elsewhere (*38*). In contrast, KO mice breathing 11% O_2 exhibited minimal to no lesions (Fig. 6C) and were virtually indistinguishable histologically from WT controls.

Recently, α-hydroxybutyrate (α-HB) was identified as a circulating plasma marker of Leigh syndrome (*39*). Consistent with this, we found that α-HB was elevated in the plasma of *Ndufs4* KO mice breathing ambient air, but not in *Ndufs4* KO mice treated with chronic hypoxia (Fig. 6D). Similarly, plasma lactate levels were increased in *Ndufs4* KO mice breathing ambient air between 50 and 65 days of age, whereas this increase was partially prevented by 11% hypoxic exposure (Fig. 6E).

Collectively, these studies confirm that chronic hypoxic exposure to breathing 11% O_2 activates the endogenous hypoxic response. Hypoxia does not correct the proximal lesion within mitochondrial complex I, but rather prevents the onset of subsequent biochemical and histopathological defects.

Discussion

The preclinical studies described here suggest that hypoxic gas mixtures may be useful in treating or preventing mitochondrial disorders. This approach is seemingly counterintuitive, because oxygen is a key substrate for the RC. However, hypoxia activates an evolutionarily conserved adaptive program that allows mammals to cope with limited oxygen levels. This program decreases an organism's reliance on mitochondrial oxidative metabolism. Such adaptive programs are not necessarily triggered by mitochondrial disease, because the hypoxic signal is absent in those cases. Moreover, hypoxia leads to a state in which oxygen delivery and consumption are simultaneously reduced, whereas in mitochondrial disease, oxygen delivery continues in the face of impaired oxygen utilization. Such a mismatch between delivery and utilization potentially contributes to oxygen toxicity. Hence, hypoxia may represent nature's solution for overcoming mitochondrial disease pathology, both by triggering innate adaptive programs and by simultaneously limiting the substrate for oxygen toxicity.

Multiple cellular and systemic mechanisms are probably acting in concert to provide the therapeutic effect we observed in mice. First, hypoxia may be triggering the HIF-dependent transcriptional program that is known to activate key biochemical pathways, including glycolysis for redox-neutral ATP production and decreased flux through PDH to prevent mitochondrial ROS generation. Second, breathing 11% O_2 reduces the provision of oxygen to the cell—oxygen that would otherwise be available as a substrate for free radical production or aberrant signaling. Many enzymes are designed to operate under reducing conditions and are highly sensitive to ambient oxygen levels. Hypoxia may establish a new oxygen set point that is better suited to the cellular environment created by impaired RC activity, whereas hyperoxia may create an environment that is less favorable. Third, it is likely that hypoxia is also operating at the level of organ systems physiology (such as O_2 delivery and CO_2 clearance by the cardiovascular system, endocrine function, and immune signaling), which are inherently non–cell-autonomous and previously reported to be altered in humans living at high altitudes. Future studies will fully decipher the role of HIF and the cellular versus cell-autonomous mechanisms underlying the in vivo therapeutic benefit.

Our results may hold therapeutic potential for patients with mitochondrial disease. However, before the chronic hypoxia strategy described here can be evaluated in the clinical setting, additional preclinical studies are needed to establish its safety and efficacy. First, studies of additional mouse models will determine the generalizability of this approach to other rare mitochondrial disorders, common disorders of mitochondrial dysfunction, and disorders of oxidative stress. Second, in the current study, we used a treatment regimen consisting of chronic 11% inspired oxygen. Healthy humans can acclimate to high altitudes such as those encountered in Mount Blanc, Peru, and Nepal, where ambient oxygen tensions are comparable to those used in our experiments, but it is possible that these conditions would not be well tolerated by patients. Future studies should thus evaluate whether intermediate oxygen levels between 11 and 20% are effective in mouse disease models. Finally, if intermittent hypoxia proves as effective as chronic hypoxia, it may allow for a nighttime therapy for which face masks and sleeping tents have already been devised by the sports industry.

An important principle in the management of mitochondrial disease is to avoid exposures, such as aminoglycoside or tetracycline antibiotics, that are known to be toxic to mitochondria. Patients with mitochondrial disease (like many other patients) are routinely treated with supplemental oxygen and breathe high levels of inspired oxygen during general anesthesia, recovery from surgery, and intensive care. Retrospective or prospective studies may help to extend our observations to humans, and if confirmed, would imply that caution should be exercised in O_2 exposure, and that administering supplemental oxygen should be limited to those instances in which it is clinically indicated.

At present, how lesions in the RC lead to such diverse pathology remains a mystery. Given the striking therapeutic efficacy of hypoxic breathing and the detrimental effect of moderate hyperoxia we saw in our studies, we propose that aberrant oxygen metabolism, signaling, or toxicity lies at the heart of mitochondrial pathogenesis. The identification of such a critical parameter suggests that a real understanding of mitochondrial pathogenesis is within reach.

Finally, it is notable that the aging process and virtually all age-related degenerative diseases are associated with secondary mitochondrial dysfunction and oxidative stress (*40*). Although antioxidants have been proposed as a strategy to alleviate these disorders by scavenging free radicals, our work suggests that simply limiting the substrate for oxygen toxicity may prove more effective. Moreover, hypoxia can trigger an adaptive program designed to decrease our body's reliance on mitochondrial oxidative metabolism. It is conceivable that breathing hypoxic gas mixtures may prevent the onset of more common disorders.

REFERENCES AND NOTES

1. P. Rich, *Nature* **421**, 583 (2003).
2. S. B. Vafai, V. K. Mootha, *Nature* **491**, 374–383 (2012).
3. W. J. Koopman, P. H. Willems, J. A. Smeitink, *N. Engl. J. Med.* **366**, 1132–1141 (2012).
4. J. Nunnari, A. Suomalainen, *Cell* **148**, 1145–1159 (2012).

5. G. Pfeffer, K. Majamaa, D. M. Turnbull, D. Thorburn, P. F. Chinnery, *Cochrane Database Syst. Rev.* **4**, CD004426 (2012).
6. N. J. Lake, M. J. Bird, P. Isohanni, A. Paetau, *J. Neuropathol. Exp. Neurol.* **74**, 482–492 (2015).
7. G. S. Gorman *et al.*, *Ann. Neurol.* **77**, 753–759 (2015).
8. S. Parikh *et al.*, *Genet. Med.* **17**, 689–701 (2015).
9. R. H. Haas *et al.*, *Pediatrics* **120**, 1326–1333 (2007).
10. O. Shalem *et al.*, *Science* **343**, 84–87 (2014).
11. T. Wang, J. J. Wei, D. M. Sabatini, E. S. Lander, *Science* **343**, 80–84 (2014).
12. M. P. King, G. Attardi, *Science* **246**, 500–503 (1989).
13. S. E. Calvo, K. R. Clauser, V. K. Mootha, *Nucleic Acids Res.* **44**, D1251–D1257 (2016).
14. M. Ohh *et al.*, *Nat. Cell Biol.* **2**, 423–427 (2000).
15. C. M. Robinson, M. Ohh, *FEBS Lett.* **588**, 2704–2711 (2014).
16. G. L. Wang, B. H. Jiang, E. A. Rue, G. L. Semenza, *Proc. Natl. Acad. Sci. U.S.A.* **92**, 5510–5514 (1995).
17. A. J. Majmundar, W. J. Wong, M. C. Simon, *Mol. Cell* **40**, 294–309 (2010).
18. M. Ivan *et al.*, *Proc. Natl. Acad. Sci. U.S.A.* **99**, 13459–13464 (2002).
19. O. Iliopoulos, A. P. Levy, C. Jiang, W. G. Kaelin Jr., M. A. Goldberg, *Proc. Natl. Acad. Sci. U.S.A.* **93**, 10595–10599 (1996).
20. P. H. Maxwell *et al.*, *Nature* **399**, 271–275 (1999).
21. D. L. Buckley *et al.*, *J. Am. Chem. Soc.* **134**, 4465–4468 (2012).
22. M. H. Rabinowitz, *J. Med. Chem.* **56**, 9369–9402 (2013).
23. N. S. Chandel *et al.*, *Proc. Natl. Acad. Sci. U.S.A.* **95**, 11715–11720 (1998).
24. Y. L. Chua *et al.*, *J. Biol. Chem.* **285**, 31277–31284 (2010).
25. I. Papandreou, R. A. Cairns, L. Fontana, A. L. Lim, N. C. Denko, *Cell Metab.* **3**, 187–197 (2006).
26. D. Tello *et al.*, *Cell Metab.* **14**, 768–779 (2011).
27. J. W. Kim, I. Tchernyshyov, G. L. Semenza, C. V. Dang, *Cell Metab.* **3**, 177–185 (2006).
28. M. C. Simon, *Cell Metab.* **3**, 150–151 (2006).
29. E. van Rooijen *et al.*, *Blood* **113**, 6449–6460 (2009).
30. B. R. Pinho *et al.*, *Br. J. Pharmacol.* **169**, 1072–1090 (2013).
31. K. D. Stackley, C. C. Beeson, J. J. Rahn, S. S. Chan, *PLOS One* **6**, e25652 (2011).
32. J. M. Harris *et al.*, *Blood* **121**, 2483–2493 (2013).
33. K. Santhakumar *et al.*, *Cancer Res.* **72**, 4017–4027 (2012).
34. R. Chowdhury *et al.*, *ACS Chem. Biol.* **8**, 1488–1496 (2013).
35. S. E. Kruse *et al.*, *Cell Metab.* **7**, 312–320 (2008).
36. I. G. Pawson, *Proc. R. Soc. London Ser. B* **194**, 83–98 (1976).
37. J. Caston, N. Jones, T. Stelz, *Neurobiol. Learn. Mem.* **64**, 195–202 (1995).
38. A. Quintana, S. E. Kruse, R. P. Kapur, E. Sanz, R. D. Palmiter, *Proc. Natl. Acad. Sci. U.S.A.* **107**, 10996–11001 (2010).
39. J. Thompson Legault *et al.*, *Cell Rep.* **13**, 981–989 (2015).
40. R. S. Balaban, S. Nemoto, T. Finkel, *Cell* **120**, 483–495 (2005).

ACKNOWLEDGMENTS

We thank W. Kaelin Jr. and members of the Mootha lab for valuable feedback; R. Sharma, M. Ferrari, A. Rogers, and the MGH animal facility for assistance with experiments; and F. van Eeden for Tg(*phd3::EGFP*) zebrafish. I.H.J. is supported by the Department of Energy Computational Science Graduate Fellowship Program (grant DE-FG02-97ER25308). N.E.S. is supported by the National Institutes of Health (NIH) through a NHGRI Pathway to Independence Award (K99-HG008171) and a postdoctoral fellowship from the Simons Center for the Social Brain at the Massachusetts Institute of Technology. F.Z. is supported by NIH through NIMH (grants 5DP1-MH100706 and 1R01-MH110049) and NIDDK (grant 5R01DK097768-03); a Waterman Award from NSF; the New York Stem Cell, Simons, Paul G. Allen Family, and Vallee Foundations; and B. Metcalfe. F.Z. is a New York Stem Cell Foundation Robertson Investigator. W.G. is supported by NIH grants R01DK090311 and R24OD017870 and is a Pew Scholar in the Biomedical Sciences. This work was supported by a gift from the Marriott Mitochondrial Disorders Research Fund (V.K.M.) and a gift in memory of Daniel Garland (V.K.M.). V.K.M. is an Investigator of the Howard Hughes Medical Institute. V.K.M. is a founder of and paid scientific advisor for Raze Therapeutics. W.G. is a paid consultant for FATE Therapeutics. F.Z. is a founder of and a scientific advisor for Editas Medicine and a scientific advisor for Horizon Discovery. V.K.M., I.H.J., L.Z., and W.M.Z. are listed as inventors on a patent application filed by Massachusetts General Hospital related to technology reported in this paper on the use of hypoxia and the hypoxia response in the treatment of mitochondrial dysfunction. F.Z., O.S., and N.E.S. are listed as inventors on a patent application (PCT/US2013/074800) filed by The Broad Institute/MIT related to the genome-scale CRISPR knockout screening technology used in this study. The CRISPR knockout library is available through a Uniform Biological Materials Transfer Agreement from Addgene. The *Ndufs4* KO mice were a kind gift of R. Palmiter and are available under a materials transfer agreement with the University of Washington, Seattle.

SUPPLEMENTARY MATERIALS

www.sciencemag.org/content/352/6281/54/suppl/DC1
Materials and Methods
Figs. S1 to S10
Tables S1 and S2
References (*41*–*44*)

14 August 2015; accepted 9 February 2016
Published online 25 February 2016
10.1126/science.aad9642

FLOW CHEMISTRY

On-demand continuous-flow production of pharmaceuticals in a compact, reconfigurable system

Andrea Adamo,[1] Rachel L. Beingessner,[2] Mohsen Behnam,[1]* Jie Chen,[1] Timothy F. Jamison,[2]† Klavs F. Jensen,[1]† Jean-Christophe M. Monbaliu,[1]‡ Allan S. Myerson,[1]† Eve M. Revalor,[1]§ David R. Snead,[2]|| Torsten Stelzer,[1]¶ Nopphon Weeranoppanant,[1] Shin Yee Wong,[1]# Ping Zhang[2]

Pharmaceutical manufacturing typically uses batch processing at multiple locations. Disadvantages of this approach include long production times and the potential for supply chain disruptions. As a preliminary demonstration of an alternative approach, we report here the continuous-flow synthesis and formulation of active pharmaceutical ingredients in a compact, reconfigurable manufacturing platform. Continuous end-to-end synthesis in the refrigerator-sized [1.0 meter (width) × 0.7 meter (length) × 1.8 meter (height)] system produces sufficient quantities per day to supply hundreds to thousands of oral or topical liquid doses of diphenhydramine hydrochloride, lidocaine hydrochloride, diazepam, and fluoxetine hydrochloride that meet U.S. Pharmacopeia standards. Underlying this flexible plug-and-play approach are substantial enabling advances in continuous-flow synthesis, complex multistep sequence telescoping, reaction engineering equipment, and real-time formulation.

Whereas manufacturing of automobiles, electronics, petrochemicals, polymers, and food use an assembly-line and/or continuous, steady-state strategy, pharmaceutical synthesis remains one of the last industrial processes to apply a noncontinuous or "batch" approach. Moreover, pharmaceutical companies generally assemble the active pharmaceutical ingredient (API) using molecular fragments obtained from different sources, with the final synthesis steps done at the company location. The API is then often mixed with excipients and formulated in the final drug product form at a separate plant. As a result, production of a finished dosage form can require up to a total of 12 months, with large inventories of intermediates at several stages. This enormous space-time demand is one of a myriad of reasons that has led to increased interest in continuous manufacturing of APIs and drug products, as well as in the development of integrated processes that would manufacture the drug product from raw materials in a single end-to-end process (*1*–*5*).

Another major challenge facing the pharmaceutical industry is drug shortages; the U.S. Food and Drug Administration (FDA) has reported well over 200 cases per year during 2011–2014 (*6*). The root causes of these shortages often trace back to factors reflective of the limitations of batchwise manufacturing, such as variations in quality control and supply chain interruption. Moreover, the small number of suppliers for any particular medicine further exacerbates the challenges faced by batchwise manufacturing to respond to sudden changes in demand or need,

[1]Department of Chemical Engineering, Massachusetts Institute of Technology, 77 Massachusetts Avenue, Cambridge, MA 02139, USA. [2]Department of Chemistry, Massachusetts Institute of Technology, 77 Massachusetts Avenue, Cambridge, MA 02139, USA.
*Present address: Nuvera Fuel Cells, 129 Concord Road, Billerica, MA 01821, USA. **†Corresponding author. E-mail: tfj@mit.edu (T.F.J); kfjensen@mit.edu (K.F.J); myerson@mit.edu (A.S.M)**
‡Present address: Department of Chemistry, University of Liège, Quartier Agora, Allée du six Août 13, B-4000 Liège (Sart Tilman), Belgium. §Present address: Department of Chemical and Biomolecular Engineering, Faculty of Medicine, Dentistry and Health Sciences, University of Melbourne, 3010 VIC, Australia. ||Present address: Georgia-Pacific Chemicals, 2883 Miller Road, Decatur, GA 30312, USA. ¶Present address: Department of Pharmaceutical Sciences, University of Puerto Rico, Medical Sciences Campus, San Juan, PR 00936, USA. #Present address: Chemical Engineering and Food Technology Cluster, Singapore Institute of Technology, 10 Dover Drive, Singapore 138683. **Present address: Novartis Institute of Biomedical Research, 250 Massachusetts Avenue, Cambridge, MA 02139, USA.

Hypoxia as a therapy for mitochondrial disease

Isha H. Jain, Luca Zazzeron, Rahul Goli, Kristen Alexa, Stephanie Schatzman-Bone, Harveen Dhillon, Olga Goldberger, Jun Peng, Ophir Shalem, Neville E. Sanjana, Feng Zhang, Wolfram Goessling, Warren M. Zapol and Vamsi K. Mootha (February 25, 2016)

Science **352** (6281), 54-61. [doi: 10.1126/science.aad9642]
originally published online February 25, 2016

Editor's Summary

Thriving on a breath of low oxygen

Mitochondrial diseases are debilitating and largely untreatable. Most are caused by genetic mutations that impair the mitochondrial respiratory chain, which generates cellular energy. Because these diseases do not affect all tissues equally, it is thought that endogenous mechanisms exist that can help cells cope with mitochondrial defects. Jain *et al.* identified the hypoxia response, a mechanism that helps cells adapt when oxygen is limited, as a potent suppressor of mitochondrial dysfunction (see the Perspective by Shoubridge). Mouse models of the mitochondrial disease Leigh syndrome showed fewer symptoms and a dramatically extended life span when raised in a hypoxic environment.

Science, this issue p. 54; see also p. 31

Science (print ISSN 0036-8075; online ISSN 1095-9203) is published weekly, except the last week in December, by the American Association for the Advancement of Science, 1200 New York Avenue NW, Washington, DC 20005.